

Contents lists available at ScienceDirect

### Journal of Catalysis

journal homepage: www.elsevier.com/locate/jcat



## Investigating the impact of micropore volume of aminosilica functionalized SBA-15 on catalytic activity for amine-catalyzed reactions



Nitish Deshpande <sup>a</sup>, Jee-Yee Chen <sup>a</sup>, Takeshi Kobayashi <sup>b</sup>, Eun Hyun Cho <sup>a</sup>, Hannah Pineault <sup>a</sup>, Li-Chiang Lin <sup>a,c</sup>, Nicholas A. Brunelli <sup>a,\*</sup>

- <sup>a</sup> The Ohio State University, William G. Lowrie Department of Chemical and Biomolecular Engineering, Columbus, OH 43210, USA
- <sup>b</sup> Ames National Lab, Iowa State University, Ames, IA 50011, USA
- <sup>c</sup> National Taiwan University, Department of Chemical Engineering, No. 1, Sec. 4, Roosevelt Rd., Taipei 10617, Taiwan

#### ARTICLE INFO

# Article history: Received 11 April 2022 Revised 19 August 2022 Accepted 17 September 2022 Available online 24 September 2022

Keywords:
Aldol reaction and condensation
Aminosilica
Knoevenagel condensation
Glucose isomerization
Micropores
SBA-15

#### ABSTRACT

Mesoporous materials such as SBA-15 are used in many applications since the materials are robust and have tunable properties. Whereas these materials are thought to be ideal, the materials are complex with the common synthesis methods producing materials that contain micropores. This work will investigate the impact of micropores on catalytic activity of aminosilica materials. For comparison, materials are formed using a standard method that produces materials with micropores (REG-SBA-15) and using a modified method that produces materials with negligible micropore volume (NMP-SBA-15). After grafting the calcined support with an aminosilane (either (N-methyl amino propyl) trimethoxy silane (denoted as 2°Am) or (N,N-diethyl-3-amino propyl) trimethoxy silane (3°Am)), catalytic testing experiments reveal that NMP-SBA-15 functionalized materials are more active than REG-SBA-15 functionalized materials for a range of reactions. The reactions include (a) glucose isomerization where amines interacting with surface silanols limit catalytic activity and (b) aldol and Knoevenagel chemistry where amine-silanol interactions increase the reaction rate. For aldol chemistry, the observed difference in rate is further investigated using site quantification experiments. Interestingly, the results reveal that three types of sites exist for each material, including sites that are (1) highly active, (2) intermediate active, and (3) inactive. NMR experiments indicate that amines immobilized on REG-SBA-15 supports are less mobile than amines on NMP-SBA-15. For REG-SBA-15, the materials are found to have aminosilanes that have limited mobility and the largest fraction of inactive sites, which suggests that the inactive catalytic sites are in the micropores. Overall, the design of highly active catalytic materials can be achieved using materials that have limited micropore volumes.

© 2022 Elsevier Inc. All rights reserved.

#### 1. Introduction

Mesoporous silica supports are robust, tunable platform materials that are attractive in many applications [1,2], including  $\rm CO_2$  capture [3,4], drug delivery [5–7], sensors [8], enzyme immobilization [9], and catalysis [10–12]. Of the different mesoporous materials, SBA-15 is commonly studied since the synthesis methods are well-established and the resulting materials have well-defined mesopores. Indeed, SBA-15 is often considered a model mesoporous support since it is a material with uniform-sized mesopores. SBA-15 has been extensively used to investigate synthesis-structure–function behavior for catalytic materials with the implicit assumption that all sites in the material have

equivalent catalytic activity [13–22]. In reality, SBA-15 is a complex material that could lead to heterogeneity in the types of sites that requires rigorous evaluation of the per site catalytic activity.

SBA-15 can be transformed into a catalyst for many reactions, including C-H functionalization [23,24], aldol chemistry [19,21], biomass conversion [25,26], and other reactions [27,28]. For these reactions, the catalyst can be prepared through different techniques and is commonly produced through grafting an organosilane onto the surface to immobilize the catalytic species into the reusable heterogeneous support. The immobilized species can be many different types of species, including organometallic complexes [23] or relatively simple aminosilanes. Aminosilane functionalization was one of the original methods to immobilize catalytic species and remains popular with the recognition that organic amines can be powerful organocatalysts [29,30]. Interestingly, aminosilane immobilization on SBA-15 places a basic amine

E-mail address: brunelli,2@osu.edu (N.A. Brunelli).

<sup>\*</sup> Corresponding author.

proximal to weakly acidic surface silanols that can interact to produce fascinating catalytic results. Indeed, the interaction of an amine with surface silanols can either inhibit the catalytic activity as has been observed for glucose isomerization [31,32] or enhance the catalytic activity through cooperative interactions [13,22,33–35].

The amine-silanol interactions can be tuned with most research focusing on tuning the surface density or structure of the aminosilane [14,36,37]. The surface density of aminosilane affects the ratio of amines to silanols present in the system [36]. As aminosilane functionalization consumes surface silanols, increasing the surface density of aminosilanes results in fewer available silanols to interact with the amine. In addition to the surface density, aminesilanol interactions are affected by the structure of the aminosilane. The structure can be tuned through controlling the linker length – the alkyl chain connecting the amine to the silicon atom in the aminosilane - or adjusting the amine substituents - the alkyl groups extending from the amine (Scheme 1). For glucose isomerization, amine-silanol interactions could be mitigated through using high densities of aminosilane to consume surface silanols [31], using a short methylene linker [31], and/or using bulky isopropyl substituents [32]. These strategies resulted in increased catalytic activity for glucose isomerization compared to the commonly used aminosilane with a propyl linker and methyl substituents.

Whereas reducing amine-silanol interactions is beneficial for some reactions, amine-silanol interactions can enhance the catalytic activity through cooperative interactions. Cooperative interactions occur when two (or more) functional groups are used in combination and result in a higher reaction rate than the individual components. For aldol chemistry, amines interacting with silanols can enable an efficient enamine mechanism [13,38-40] since silanols are weakly acidic and high activity is achieved when using weak acids, including alcohols [15,20,41]. Compared to using alcohols, surface silanols are beneficial cooperative partners as they are inherently part of the silica surface provided that surface coverages of aminosilane are less than a monolayer [36,37]. The cooperative interaction can be tuned through adjusting the design of the aminosilane. For efficient cooperativity for aldol chemistry, the aminosilane should have a propyl linker since shorter linkers result in lower catalytic activity [14,42]. Additionally, the amine can be either a primary or secondary amine with primary amines being more active than secondary amines in water [39]; secondary amines are more active than primary amines in commonly used solvents such as acetone and will be used for aldol chemistry in this work.

$$\begin{array}{c}
R_{1} \\
R_{1} - N \\
O - Si \\
O O -
\end{array}$$

**Scheme 1.** Aminosilane structure with a tunable alkyl linker length (n) and substituent size  $(R_1, R_2)$ .

The interaction of amines and surface silanols represents an important design metric that can be probed through measuring the molecular mobility. Molecular mobility and correspondingly amine-silanol interactions can be probed through using advanced 2D solid state NMR experiments [43]. The experiments involve measuring the <sup>13</sup>C cross-polarization (CP) SS NMR spectrum with different CP times. CP experiments use excitation of the hydrogen (<sup>1</sup>H; proton) followed by transfer of polarization to the carbon (<sup>13</sup>C) through a CP pulse. The CP pulse length can be varied and is known to affect the polarization transfer [43]. Species that can move more freely on the surface are expected to necessitate longer CP times than species where strong amine-silanol interactions limit mobility. This was demonstrated previously using non-basic organosilanes, which did not interact with the surface, that had CP build up times for the third carbon from the siloxy tether of 119 us [43]. For basic aminosilanes, a shorter CP build up time of  $\sim$  33 us was measured for the third carbon most distant from the siloxy tether, indicating that the amine had sufficient flexibility to interact with the surface.

Although the idealized depiction of SBA-15 has enabled investigation of synthesis structure-reactivity relationships, the most common synthetic conditions for SBA-15 (Fig. S1) also produce a secondary micropore network [44,45] that may impact the material performance. Nitrogen physisorption data and other characterization methods reveal that the structure can contain micropores that account for as large as  $\sim$ 30% of the overall pore volume [45]. The presence of micropores has the potential to impact the amine-silanol interactions, making it desirable to tune the synthesis conditions to produce materials with limited to no micropore volume. The micropore volume of SBA-15 can be tuned through adjusting the synthesis conditions. Whereas many parameters can be tuned [46-51], the micropore volume can be reduced through modifying the temperature. SBA-15 is synthesized through using a two-step hydrothermal method using a low temperature (T<sub>1</sub>) for 24 h before heating to a higher aging temperature  $(T_2)$ . The most common method  $(T_1 = 40 \, ^{\circ}\text{C} \text{ and } T_2 = 100 \, ^{\circ}\text{C})$  produces a material with micropores since the ends of the polymer (PEO domains) protrude into the walls of the silica [52.53]. Interestingly, the micropore volume can be reduced by using a higher T<sub>2</sub> of 130 °C [45]. Whereas a T<sub>2</sub> of 100 °C is used for the practical reason that it does not require a sealed reactor to limit water evaporation, this practical choice has implications that need to be understood.

The impact of the micropores of SBA-15 has received limited attention [16,54,55] even though they could have significant implications on catalyst activity. Researchers have synthesized catalytic materials with different micropore volumes for use in the aldol reaction and condensation. The Jentoft group [16] investigated the impact of micropores on catalytic activity for the aldol reaction and condensation for sulfonic acid functionalized silica. Although the sulfonic acid sites functionalized on supports with different amounts of micropores had similar average catalytic activity, the per site catalytic activity was not quantified. Additionally, these sulfonic acid catalysts tend to be less active than amine functionalized materials since sulfonic acids and silanols do not cooperatively catalyze the reaction. Our recent work has demonstrated that aminosilica materials with limited to no micropores (NMP-SBA-15) are more active for aldol chemistry [55] and the Knoevenagel condensation [54]. Yet, the underlying difference in catalytic activity has not been investigated to establish the molecular basis for the observed difference.

The goal of this work is to investigate the impact of micropores on catalytic activity for aminosilica materials. Materials will be synthesized with a range of textural properties, including different micropore volumes. The materials will be functionalized using post-synthetic grafting and will be characterized using standard

techniques. The materials will be tested in a range of catalytic reactions to assess differences in catalytic activity. The underlying differences in catalytic activity will be investigated using site quantification experiments to determine differences in the fraction and types of active sites. The different materials will be characterized using advanced NMR method to quantify the crosspolarization time constants ( $T_{CH}$ ) to demonstrate differences in aminosilane mobility that are used to provide insights on differences in the aminosilane location. The combined results will provide guidance on how to create highly active catalysts.

#### 2. Experimental methods

#### 2.1. Chemicals

The chemicals are used as received with the exception of toluene (ACS grade, Macron Fine Chemicals) that is dried using an MB-SPS DriSolv system (MBraun Inc.). The other chemicals include: tetra ethyl ortho silicate (TEOS; 98%, Acros Organics), hydrochloric acid (36.5-38.0% by wt., reagent grade, J. T. Baker), poly(ethylene glycol)-block-poly(propylene glycol)-block-poly (ethylene glycol) PEG-PPG-PEG, Pluronic® P-123 (Sigma-Aldrich), (N,N-diethyl-3-aminopropyl) trimethoxysilane (Gelest), (Nmethylaminopropyl) trimethoxysilane (Gelest), ethanol (200 proof. Decon Labs Inc.), n-hexanes (95%, HPLC grade, Millipore), dextrose (USP grade, Fisher), D-(+)-mannose (99%, Alfa Aesar), D-fructose (99%, Alfa Aesar), D-mannitol (USP grade, Amresco), benzaldehyde (98%, Bean Town Chemical), malononitrile (99%, Bean Town Chemical), 4-nitrobenzaldehyde (98%, Aldrich), acetone (HPLC grade, Fisher), methane sulfonic acid (MSA; Alfa Aesar), diethylene glycol dibutyl ether (>98%, TCI), 1,3,5-trimethoxybenzene (>98%, TCI), cetyltrimethylammonium bromide (high purity grade, Amresco), sodium hydroxide (ACS grade, GFS Chemicals), and deuterated chloroform (99.8% isotopic with 0.03% TMS, Bean Town Chemical). Deionized (DI) water is from a house supply of Milli-Q quality water.

## 2.2. Material synthesis, material characterization, and naming convention of catalytic materials

For many of the synthesis methods and characterization methods, the details of these experimental procedures are reported in the supplemental information. A range of synthesis procedures are used to produce mesoporous materials with different textural properties, including regular pure silica SBA-15 (REG) [14,15,56], pure silica SBA-15 with negligible micropores (NMP) [45,54,55], and mesoporous nanoparticles (MSN) [57]. SBA-15 is the primary support tested since it has greater hydrothermal stability than MCM-41 [58-60]. The materials are functionalized using aminosilanes - organosilanes containing an amine functional group using previously reported methods [31,32]. The grafted aminosilanes include (N-methyl amino propyl) trimethoxy silane (denoted as 2°Am) or (N,N-diethyl-3-amino propyl) trimethoxy silane (3°Am). At each stage of the synthesis, the materials are characterized using different techniques, including elemental analysis (EA), nitrogen physisorption (Figs. S2, S4, S5), SEM (Fig. S3), thermal gravimetric analysis (TGA; Fig. S6, S7), and diffuse reflectance infrared Fourier transform spectroscopy (DRIFTS; Fig. S8). The naming convention used for the materials involves the organosilane identifier (either 2°Am or 3°Am), the type of silica support (REG, NMP, or MSN), and the actual organosilane loading. For a conventional SBA-15 material functionalized with 3°Am and having an actual loading of 0.85 mmol  $g^{-1}$ , the material is labeled 3°Am-REG-0.85.

#### 2.3. Pore size reduction using hexamethyldisilazane treatment

Similar to the grafting procedure, the pore size of NMP-SBA-15 is reduced through sequential treatments with hexamethyldisilazane (HMDS). One gram of bare support silica is dried under reduced pressure (<20 mTorr) at 130 °C for 15 h in a 100 mL round-bottom flask. After degassing, the flask is attached to a Schlenk line for 30 min of cooling while purging with nitrogen flow through a septum. After purging with nitrogen, dry toluene solvent (25 mL toluene per 1 g silica) is added into the flask and is dispersed with stirring at 25 °C. The HMDS (5 times excess of the silanol groups on the silica surface [61]) is premixed with 10 mL of dry toluene and added dropwise to the silica mixture. After 24 h, 20 µL of distilled water is injected into the mixture. The flask is then attached to a septum-sealed condenser, and the temperature is increased to 80 °C under nitrogen purging. The purging is stopped once the mixture reached 50 °C and maintained at 80 °C for another 24 h with stirring. At this time, the mixture is cooled to room temperature. The mixture is filtered, washing with 300 mL of toluene, 300 mL of pure hexane, and 300 mL of ethanol. The solids are dried under reduced pressure for 15 h before calcining the material at 550 °C to remove the residual organic. The surface modification with HDMS is repeated until the mesopore size measured using the BdB-FHH model from nitrogen physisorption is similar to the mesopore size of REG-SBA-15.

#### 2.4. Determination of cross polarization time constants $(T_{CH})$

Solid-state NMR experiments are performed on an Agilent DDR2 spectrometer, equipped with a 5 mm magic angle spinning (MAS) probe and operated at 9.4 T. The samples are packed in MAS zirconia rotors and spun at 8 kHz. The mobilities of N, N-diethylaminopropyl (3°Am) groups grafted on the silica surfaces are compared among the samples through the "build-up" of <sup>13</sup>C signals during the CP period.

The  $^{13}$ C{ $^{1}$ H} CPMAS spectra are obtained using the magnitude of the RF magnetic field applied to H spins,  $v_{RF}^{H}$  = 50 kHz for  $\pi/2$  pulse and for SPINAL-64 heteronuclear decoupling during NMR signal acquisition,  $v_{RF}^{H}$  = 40 kHz during CP,  $v_{RF}^{C}$  = 48 kHz during CP. Spectra (15 for each) are acquired for each sample by varying CP contact time  $\tau_{CP}$  from 10  $\mu$ s to 1000  $\mu$ s with 6400–9600 scans for each spectrum with a 1.5 s of recycle delay.

#### 2.5. Catalytic testing

The materials are tested for catalytic activity in three different reactions, including the Knoevenagel condensation [54], the aldol reaction and condensation [13–15], and glucose isomerization [31,32]. The methods are similar to those reported previously. The details of the methods are presented in the supplemental information. Importantly, the results have been evaluated for mass transfer limitations and have shown no mass transfer limitations as previously demonstrated for glucose isomerization [31], the Knoevenagel condensation [54], and aldol chemistry (Supplemental information; Section S5, Fig. S9, and Table S2).

## 2.6. Site quantification experiments for aldol reaction and condensation

Site quantification experiments are performed using a method similar to aldol catalytic testing. The site quantification experiments differ from catalytic testing in that the required amount of catalyst is first weighed and added to an oven-dried 2N round bottom flask. A separate solution of methane sulfonic acid (MSA; 5–50  $\mu$ L) in ethyl acetate (1–1.8 mL; selected as solvent because pure

ethyl acetate had limited to no impact on catalytic activity; see supplemental information S7) is prepared using micropipettes. A predetermined amount (between 5 and 50  $\mu$ L) of this solution is added to the catalyst using micropipettes to obtain the desired methane sulfonic acid (MSA):amine ratio. The mixture is allowed to mix slowly (~200 RPM) for 60 s before adding 2 mL of the bulk aldol reaction solution to it. A  $t_0$  sample is drawn in the first 15 s and the round-bottom flask is attached to a septum-sealed condenser under an active purge of nitrogen. The round-bottom is then lowered into the pre-heated oil bath (T = 50 °C), and the remainder of the experiment is carried out similar to a typical Aldol experiment.

#### 3. Results and discussion

#### 3.1. Material synthesis

The impact of micropores in SBA-15 is studied through synthesizing mesoporous silica supports that contain different quantities of micropores: REG-SBA-15 produced using a common synthesis method and NMP-SBA-15 produced using a modified procedure that involves increasing the aging temperature from 100 °C to 130 °C [45]. The materials are characterized using nitrogen physisorption and SEM (Fig. S3). As shown in Fig. 1, nitrogen physisorption is used to investigate the textural properties of the materials. For REG-SBA-15, the data are consistent with a Type IV isotherm with a H1 hysteresis loop; the material has a total surface area of 920 m $^2$  g $^{-1}$ , similar to previous syntheses of SBA-15 [37,56]. Using the t-plot method, the micropore volume is determined to be 0.07 cm<sup>3</sup> g<sup>-1</sup>, consistent with a material with micropores. For NMP-SBA-15, the nitrogen physisorption isotherm is also a Type IV with an H1 hysteresis loop, but the material has a smaller total surface area of 530 m<sup>2</sup> g<sup>-1</sup>. Similar to previous reports [45], the modified synthesis method for NMP-SBA-15 produces a material with a micropore volume of  $0.02 \text{ cm}^3 \text{ g}^{-1}$ , which is substantially lower than the micropore volume of REG-SBA-15 (0.07 cm $^3$  g $^{-1}$ ).

After calcination, the materials are grafted with N,N-diethyl amino propyl triethoxy silane (3°Am) or N-methyl amino propyl triethoxy silane (2°Am). The quantity of aminosilane grafted on

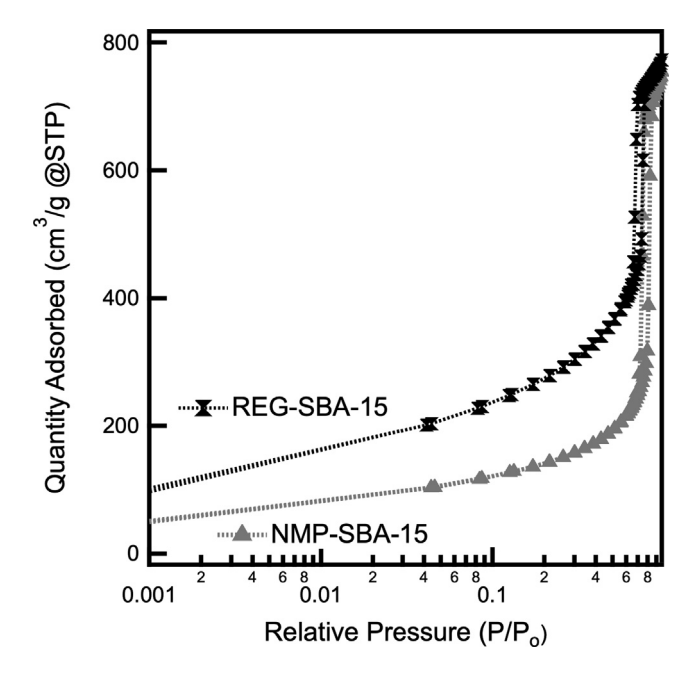


**Fig. 1.** Comparison of the nitrogen physisorption isotherms of REG-SBA-15 and NMP-SBA-15.

the material is calculated from elemental analysis data. For 2°Am grafted onto REG-SBA-15, it is determined that the nitrogen content is 0.63 wt% N; this corresponds to a loading of 0.45 mmol N  $g^{-1}$ (material is labeled 2°Am-REG-0.45). For comparison, the goal is to functionalize NMP-SBA-15 with a similar amount of aminosilane with the choice being to maintain either surface loading - mmol N  $\rm g^{-1}$  – or surface density –  $\mu \rm mol~N~m^{-2}$ . For the aldol reaction and condensation, previous work [36] has shown that the surface density of aminosilanes is important since the amines and surface silanols can cooperatively catalyze the reaction. Therefore, all materials will be made using a similar target surface density of 0. 48  $\mu$ mol N m<sup>-2</sup>, which is the loading of 2°Am-REG-0.45. For NMP-SBA-15 functionalization, the quantity of aminosilane in the functionalization mixture is adjusted to achieve the desired surface density. The resulting material is determined to have a surface loading of 0.31 mmol N g<sup>-1</sup> (2°Am-NMP-0.31).

After organosilane functionalization, the materials are characterized using nitrogen physisorption to determine the textural properties. Interestingly, 2°Am organosilane functionalization of REG-SBA-15 significantly reduces the micropore volume from 0.07 cm³ g⁻¹ to 0.03 cm³ g⁻¹, as shown in Fig. S4. The data suggest that a portion of the aminosilane is functionalized in the micropores or blocks the micropores. This behavior appears to be a general phenomenon since a large survey of literature has reported similar data [18,41,62], but the catalytic implications have not been rigorously assessed for aminosilica materials. For NMP-SBA-15, the data indicate only a small reduction in the low-pressure nitrogen uptake, as the material has limited micropore surface area and volume before grafting.

## 3.2. Testing for catalytic activity for the aldol reaction and condensation

The functionalized materials are tested for catalytic activity in the aldol reaction and condensation through monitoring the time-dependent conversion of 4-nitrobenzaldehyde reacting with acetone. For 2°Am-REG-0.45, the material converts the 4nitrobenzaldehyde with first order kinetics, as shown in Fig. 2. The observed conversion over time is similar to previous reports for SBA-15 and is not mass transfer limited, as shown in the supplemental information (Section S5, Fig. S9, and Table S2). Interestingly, 2°Am-NMP-0.31 achieves higher conversion in the same amount of time, demonstrating that the catalyst has a higher average per site activity. This is consistent with our recent work for other reactions [54,55]. The data are used to calculate the reaction rate constant for both materials. It is determined that  $k_{obs} = 0.22 \, h^{-1}$ for  $2^{\circ}$ Am-REG-0.45 and 0.35 h<sup>-1</sup> for  $2^{\circ}$ Am-NMP-0.31. The  $2^{\circ}$ Am-NMP-0.31 material is observed to have a higher rate constant than 2°Am-REG-0.45 by a factor of 1.6.

The observed difference in reaction rate could either be associated with (1) a different fraction of sites or (2) different types of sites that have different activity. These differences are investigated through using a series of site quantification experiments. The experiments involve adding a fixed amount of methane sulfonic acid (MSA;  $pK_a = -2$ ) relative to the amount of amine (MSA:2°Am) to selectively poison a fraction of the catalytic sites and then measuring the rate of reaction. These experiments are repeated for a range of MSA:2°Am. These data are used to quantify the fraction of active sites by determining the intercept of the reaction rate constant data with the x-axis. Also, the data are used to determine if the catalyst has multiple types of active sites since the data will have a corresponding number of slopes.

The site quantification experiments are performed for 2°Am-REG-0.45. As shown in Fig. 3, the observed TOF decreases monotonically toward the x-axis. Fitting the data with a line, it is possible to determine that the fraction of active sites is 0.33 of the total

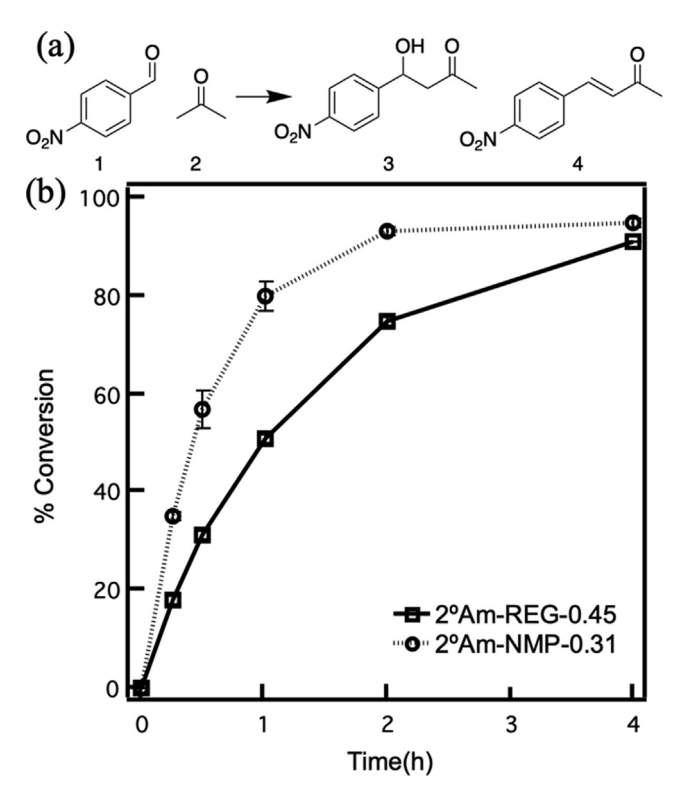


**Fig. 2.** (a) Schematic of the aldol reaction and condensation combining 4-nitrobenzaldehyde (1) with acetone (2) to produce a beta keto-alcohol (3) and an ene-one (4). (b) Comparison of conversion of 4-nitrobenzaldehyde over time for different catalysts. Testing is performed using 3 mol% amine at 40 °C. The products are formed in a ratio of 86:14 for the reaction (3):condensation (4) products.

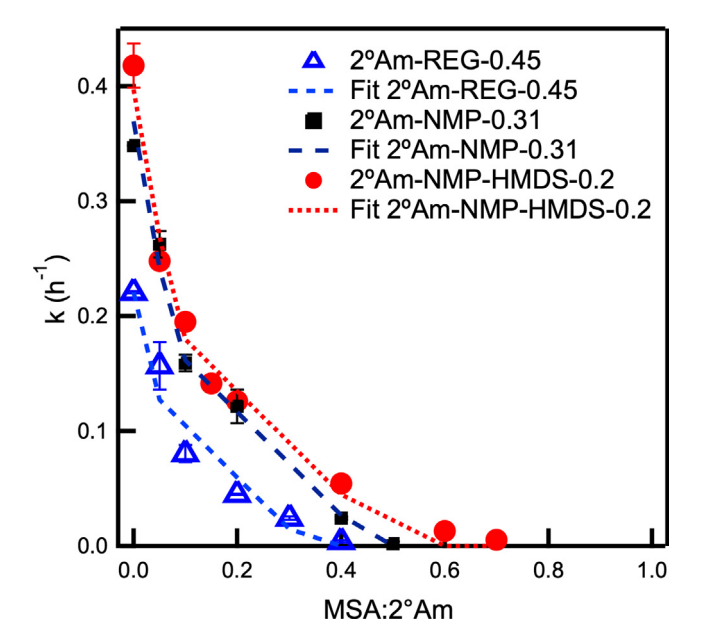


**Fig. 3.** Comparison of the observed reaction rate constant for the aldol reaction and condensation for REG-SBA-15 and NMP-SBA-15 as a function of the amount of methane sulfonic acid:amine (MSA:2°Am). Catalytic testing is performed using 3 mol% amine for the aldol condensation/reaction between 4-nitrobenzaldehyde adcetone at 40 °C. The error bars represent the standard deviation of the kinetic data for multiple catalytic tests. The experimental data are fit using a three-site model.

amines (based on elemental analysis). The data indicate that at least two types of sites exist since a fraction of sites are not active. This nullifies the hypothesis that all sites have equal catalytic

activity. Interestingly, the site quantification experiments reveal that 2°Am-NMP-0.31 has a fraction of active sites of 0.46. This fraction of sites is a factor of 1.4 greater than the fraction of sites in 2°Am-REG-0.45, demonstrating that the difference in the catalytic activity can be attributed to the fraction of active sites.

Moreover, the site quantification experiments reveal that the material has more than two types of active catalytic sites; the rate data have different slopes at low and intermediate fractions of MSA:2°Am. The change in slope is consistent with two types of sites that are active in the material in addition to the sites that are inactive. The rate data can be fit using a three-site model:

$$k_{obs} = (f_1 k_1 + f_2 k_2 + f_3 k_3) \tag{1}$$

where  $k_{obs}$  is the observed reaction rate constant for a first order reaction,  $f_n$  is the fraction of sites of type n, and  $k_n$  is the first order rate constant for site n. Using a least squares fit program in MATLAB, the site quantification data are fit using the three-site model. Since it is assumed that the third site is inactive,  $k_3$  is set to zero. As shown in Fig. 3, the data for both 2°Am-NMP-0.31 and 2°Am-REG-0.45 are fit well by the three-site model, indicating that the same three different types of sites exist in both materials. Accordingly, changes in textural properties are not affecting the types of sites present, but the changes are affecting the fraction of sites. For the active sites, the reaction rate constant is  $2.6 \pm 0.4 \, h^{-1}$  for the highly active site and is  $0.45 \pm 0.06 \, h^{-1}$  for the intermediate active site. Intriguingly, a material comprised of only highly active sites would increase the rate of reaction by an order of magnitude compared to current materials.

The fraction of each type of active sites is different for the two materials tested. For  $2^{\circ}$ Am-REG-0.45, the fit to the site quantification data reveals that the fraction of highly active sites is 0.03  $\pm$  0.01 whereas the fraction of intermediate active sites is 0.30  $\pm$  0.04 for a fraction of total active sites of 0.33, as shown in Table 1. For  $2^{\circ}$ Am-NMP-0.31, the fraction of highly active sites is 0.08  $\pm$  0.01, and the fraction of intermediate active sites is 0.38  $\pm$  0.04. Compared to  $2^{\circ}$ Am-REG-0.45, it is shown that  $2^{\circ}$ Am-NMP-0.31 has more than twice the fraction of highly active sites and more intermediate active sites.

The fraction of active sites is used to calculate the turnover frequency (TOF) for the materials. The TOF is determined to be higher for 2°Am-NMP-0.31 (TOF = 27) than 2°Am-REG-0.45 (TOF = 22). The observed difference can be attributed to the increased fraction of highly active sites in the material as well as the increased fraction of sites. Indeed, it is determined that  $f_1/f_2$  for 2°Am-NMP-0.31 is 0.21 whereas 2°Am-REG-0.45 has a value of 0.10. The higher  $f_1/f_2$  fraction for 2°Am-NMP-0.31 compared to 2°Am-REG-0.45 likely explains the increased TOF for the material. This indicates that reducing the micropore volume increases the fraction of highly active catalytic sites.

The origin of the observed difference in catalytic activity could be associated with the micropores or the pore size. Indeed, NMP-SBA-15 has a pore size of 9 nm whereas REG-SBA-15 has a pore size of 7.1 nm. Although previous work with aminosilica catalysts [13] indicated that the mesopore size had limited to no impact on the observed catalytic activity, the previous results are based on the assumption that all sites have equal catalytic activity. Accordingly, a synthetic target became the synthesis of a material with limited to no micropores and a similar pore size as REG-SBA-15. The pore size of NMP-SBA-15 is reduced through five iterations of HMDS capping and calcining the material to produce NMP-SBA-15-HMDS. From nitrogen physisorption (Fig. S11), NMP-SBA-15-HMDS has a pore size of 7.1 nm (Fig. S12) - approximately equivalent to pore size of REG-SBA-15 of 7.1 nm - and a micropore volume of 0.01  $cm^3$   $g^{-1}$  – less than even NMP-SBA-15 (0.02  $cm^3$ g<sup>-1</sup>). After calcination, NMP-SBA-15-HMDS is functionalized with a secondary aminosilane to produce 2°Am-NMP-HMDS-0.2.

**Table 1**Calculated fitting parameters from a three-site model for REG and NMP-SBA-15.

	$f_1 (k_1 = 2.6 \pm 0.4)$	$f_2 (k_2 = 0.45 \pm 0.06)$	$f_1/f_2$	TOF (hr <sup>-1</sup> )
2°Am-REG-0.45	0.03 ± 0.01	$0.30 \pm 0.04$	0.10	22
2°Am-NMP-0.31	0.08 ± 0.01	$0.38 \pm 0.04$	0.21	27
2°Am-NMP-HMDS-0.2	$0.08 \pm 0.01$	$0.42 \pm 0.05$	0.19	27

The functionalized material is tested for catalytic activity in the aldol reaction and condensation. Interestingly, 2°Am-NMP-HMDS-0.2 exhibits the highest catalytic activity of the materials tested, as shown in Fig. 3. From the textural characterization data, the main difference between REG-SBA-15 and NMP-SBA-15-HMDS is the micropore volume. Accordingly, the data support that reducing the micropore volume results in a catalyst that is highly active.

The materials are also characterized using site quantification experiments. The site quantification experiments reveal that  $2^{\circ}\text{Am-NMP-HMDS-}0.2$  has a fraction of  $0.08 \pm 0.01$  of highly active sites and  $0.42 \pm 0.05$  intermediate activity sites with a total fraction of active sites of 0.50. Of the materials tested,  $2^{\circ}\text{Am-NMP-HMDS-}0.2$  has the highest fraction of active sites and correspondingly the highest catalytic activity. Further, these results also indicate that each material has similar types of sites. Indeed, the three-site model could be used to fit the experimental data for the different materials using the same values for the reaction rate constants for each material.

The materials are further investigated to elucidate insights on the underlying characteristics of the different sites. Whereas ongoing work is investigating the origin of the highly active and intermediate active sites to provide synthetic targets for creating highly active materials, it is also desirable to identify the structure or location of the inactive sites. The site quantification experiments reveal that the fraction of inactive sites is the highest for the bare support material that has the highest micropore volume. This suggests that the inactive sites could be located in the micropores and may indicate that the site is inaccessible. Indeed, molecular dynamic (MD) simulations (described in the SI) suggest that the aminosilanes will preferentially graft to the silica surface in the micropore. The small diameter of the micropores has the potential to impact how the amine interacts with surface silanols.

The interaction of the amines with the surface silanols is investigated through using solid-state NMR measurements. The NMR experiments involve determining the  ${}^{1}H \rightarrow {}^{13}C$  CP time constants  $(T_{CH})$  for individual carbons in the grafted aminosilanes. The  $T_{CH}$ values depend on the effective (distance- and mobilitydependent) 1H-13C magnetic dipole-dipole interactions and can provide information about the degree of atomic-level motions of silica-bound amines and their interactions with the surface [43]. To facilitate the measurements, calcined mesoporous materials are functionalized with the tertiary amine (N,N-diethylamino-3propyl trimethoxy silane) to produce 3°Am functionalized materials at the loadings listed in Table S1. The 3°Am increases the signal since the amine contains two alkyl substituents that will be the basis for comparison. The carbons in the aminosilane are labeled C<sub>1</sub>, C<sub>2</sub>, C<sub>3</sub>, C<sub>4</sub>, and C<sub>5</sub>, as shown in Scheme 2. For these materials, the  $T_{CH}$  values are derived by measuring the 'build-up' of <sup>13</sup>C mag-

$$= Si C_1 C_3 C_4 C_5$$

$$C_4 C_5$$

**Scheme 2.** 3°Am functionalized on silica with the carbon atoms numbered starting from silicon, as used in Table 1.

netizations during the CP period, as detailed in the SI. It is difficult to determine the  $T_{CH}$  for  $C_5$  since the chemical shift of  $C_5$  aligns with the chemical shift of  $C_1$ . As such, a comparison is made between the  $T_{CH}$  values of the second most distal carbon from the surface (i.e.,  $C_4$ ).

The  $T_{CH}$  value is reflective of the length of time it takes to transfer energy from the proton to the carbon. Mobile carbons will have a larger  $T_{CH}$  than immobile carbons that are adjacent to an amine interacting with the surface [43]. The range of expected  $T_{CH}$  values can be determined through analyzing materials with different surface loadings. For the high loading of 3°Am-REG-1.46, silanols are nearly absent since they are almost completely consumed by the aminosilane functionalization, reducing amine-silanol interactions and creating more mobile  $C_4$  atoms that have a  $T_{CH}$  of 55  $\mu$ s. For the low surface loading of 3°Am-REG-0.52, silanols are available for amine-silanol interactions, resulting in a  $T_{CH}$  for  $C_4$  of 33  $\mu$ s. These measurements establish the range of  $T_{CH}$  values for mobile  $C_4$  (55  $\mu$ s) and immobile  $C_4$  (33  $\mu$ s).

As the  $T_{CH}$  values are affected by the surface loading, the measurements for different materials are carried out for samples with a similar surface density of organosilanes of  $\sim\!0.95~\mu mol~N~m^{-2}$ . At this surface density, silanols are available for the amine to interact. For the 3°Am-REG-0.85 material, the  $T_{CH}$  for C<sub>4</sub> is 38  $\mu$ s, as reported in Table 2. This value implies that on the NMR time scale, which in this case is defined by the inverse of the <sup>13</sup>C-<sup>1</sup>H dipolar coupling (i.e.,  $\sim$ (20 kHz)<sup>-1</sup>), the mobility of most 3°Am groups in the sample are significantly restricted. Interestingly, the T<sub>CH</sub> value of C<sub>4</sub> measured for 3°Am-NMP-0.75 is considerably higher, suggesting increased local mobility. The results suggest that the organosilanes graft in different locations in REG-SBA-15 and NMP-SBA-15. Since REG-SBA-15 has micropores in which MD indicates the aminosilanes would functionalize, a small pore material (MSN) is synthesized, functionalized with tertiary amine (3°Am-MSN-0.96), characterized (see Fig. S5, Table S1), and analyzed with NMR. For  $3^{\circ}$ Am-MSN-0.96, the  $T_{CH}$  value for  $C_4$  is 39  $\mu$ s, reflective of the amines being immobile because of amine-silanol interactions in the small pores of the MSN material. The results are consistent with the hypothesis that the aminosilanes for 3°Am-REG-0.85 are preferentially located in the micropores.

The combined catalytic results and NMR characterization results can be used to infer information about the different types of sites. The inactive sites appear to be aminosilanes that are preferentially functionalized in the micropores. Indeed, REG-SBA-15 has the largest quantity of micropores, and NMR results for REG-SBA-15 are consistent with the aminosilanes being located in the micropores. Additionally, materials with limited micropores (NMP-SBA-15 and NMP-SBA-15-HMDS) have the lowest fraction of inactive sites.

For the active sites, the catalytic data and NMR results provide less clarity about the differences between these two sites, but it is possible to speculate that the potential differences could be associated with either the type of silanol involved in the cooperative interaction, clustering on the surface, or the location in the mesopore. It is likely that the location (i.e., external surface vs mesopores) is not responsible for two types of sites since mass transfer calculations, catalytic tests, and recent work [63] using non-porous silica demonstrate mass transfer does not impact the observed reaction rates. Additionally, aminosilane could form

**Table 2** Average cross polarization time constants ( $T_{CH}$ ) in  $\mu$ s for different carbons of 3°Am functionalized at similar surface densities on REG-SBA-15, NMP-SBA-15, and MSN.

Material	T <sub>CH</sub> (μs)		Amine-Silanol Interactions? b	
	C <sub>2</sub>	$C_3$	$C_4$	
3°Am-REG-0.52	34	21	33	Y
3°Am-REG-1.46	32	30	55	N
3°Am-REG-0.85	25	24	38	Y
3°Am-MSN-0.96	30	28	39	Y
3°Am-NMP-0.75	48	34	58	N

 $<sup>^{</sup>a}T_{CH}$  are not reported for  $C_1$  and  $C_5$  due to the overlap of their respective peaks in the  $^{13}$ C spectra.  $^{b}$  Based on value of  $T_{CH}$  of  $C_4$ .

clusters since it is known that unpromoted amines have lower activity. It is unlikely that the high active site is associated with paired (i.e., clusters of two aminosilanes) sites that have been implicated in sulfonic acid functionalized materials [64] since the role of two amines in the mechanism is unclear. However, additional work will demonstrate that materials with high densities of amines have a distinct activity from active site 1 and active site 2 [63]. Whereas the difference between the highly active and intermediate active sites is likely not the location in the mesopore or the formation of clusters, it is possible that different types of silanols could affect the observed rates. The silica surface is known to consist of different type of silanols, including isolated, vicinal, and geminal. These silanols have different acidities. As previous work has established that higher activity can be achieved using weaker acids as the cooperative partner [15,41], it is possible that the amines are interacting with different types of silanols and are promoted to different degrees.

The materials are investigated using DRIFTS to determine if differences in synthesis temperature impacted the quantity and type of silanols since synthesis conditions (i.e., HCl concentration) have been reported to have an impact [65]. Fig. S8 shows the hydroxyl

(a) N H<sub>2</sub>O (b) N H<sub>2</sub>O (b) N H<sub>2</sub>O (c) N

**Fig. 4.** (a) Schematic of the Knoevenagel condensation combining benzaldehyde (5) with malononitrile (6) to produce a condensation product (7) and water. (b) Comparison of conversion of benzaldehyde over time for different catalysts. Testing is performed using 10 mol% amine at 30 °C.

region of the DRIFTS spectra for the bare and functionalized materials. Both NMP-SBA-15 and REG-SBA-15 exhibit a sharp peak around 3740 cm<sup>-1</sup> that can be attributed to isolated silanols as well as a broad peak around 3550 cm<sup>-1</sup> that are consistent with vicinal silanols. These spectra for the bare materials are similar with differences in intensity likely associated with the difference in surface area of the materials. The similarity suggests that the synthesis temperature has limited impact on the quantity and types of silanols when normalized by surface area. After grafting, the sharp peak associated with isolated silanol decreases for both 2°Am and 3°Am materials. It is not clear how vicinal and isolated silanols interact with the amines, but it could be key to understanding the different types of sites present in the material.

As the quantity of micropores in the material impacts the fraction of catalytic sites, reducing the quantity of micropores could be a general method to improve the catalytic activity for reactions where amine silanol interactions are beneficial such as the Knoevenagel [21,22,54] or detrimental such as glucose isomerization [31,32]. For the Knoevenagel condensation, the reaction between benzaldehyde (5) and malononitrile (6) to form 2-benzylidenemalononitrile (7) serves as a probe reaction (Fig. 4a). Whereas 3°Am-REG-0.52 achieves 50% benzaldehyde conversion in one hour, 3°Am-NMP-0.38 converts 85% of benzaldehyde (Fig. 4b) in the same amount of time. These results demonstrate that the presence of micropores in REG SBA-15 negatively impacts

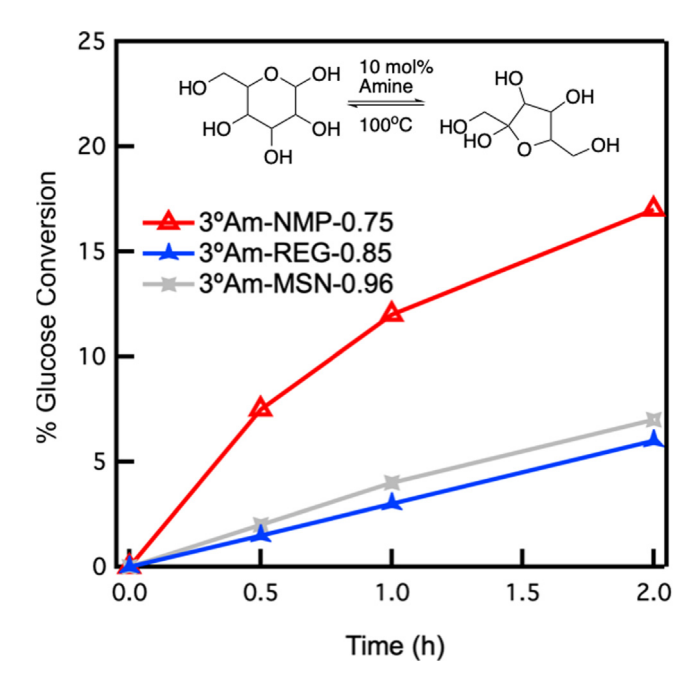


**Fig. 5.** Conversion of glucose for 3°Am grafted NMP, REG, and MSN catalysts at similar surface densities. All tests are performed using 10 mol% amine at 100 °C with a 10 wt% solution of glucose.

the catalytic activity of cooperative amines functionalized on silica supports for the Knoevenagel condensation.

The catalytic activity of tertiary amine functionalized materials is also tested in the isomerization of glucose to fructose (Fig. 5). For this reaction, recent work has demonstrated that interactions of amines with silanols reduce the initial turnover frequency (TOF<sub>0</sub>) [31,32]. Therefore, materials functionalized with similar surface densities of amines are compared. When using the same mole percent of amines added and materials with similar surface densities, the catalysts 3°Am-REG-0.85 and 3°Am-MSN-0.96 exhibit similar catalytic activity for glucose isomerization with conversion increasing over time. The conversion profile is similar to other catalysts that had limited catalytic activity for glucose isomerization [31]. Interestingly, the NMP material (3°Am-NMP-0.75) achieves higher glucose conversion with an initial turnover frequency (TOF<sub>0</sub>) that is nearly 3-fold higher than the REG SBA-15 and MSN based catalysts. As shown in Table S6, the 3°Am-NMP-0.75 material achieves a higher fructose yield at all times than the other two catalysts with a selectivity to fructose of 78% (2 h data point) that is comparable to our previous work [31,32]. Overall, the results demonstrate the benefit of reducing the micropore volume for reactions where surface silanols either positively or negatively impact the reaction.

#### 4. Summary

The impact of textural properties is investigated for aminosilica in a range of catalytic reactions. Materials are produced with a controlled quantity of micropore volume and are functionalized using aminosilanes. For the aldol reaction and condensation, it is determined that materials with limited to no micropores are more active than materials made using the conventional material synthesis. The observed difference is not associated with the mesopore size, consistent with previous work [37]. Site quantification experiments reveal that the same three types (i.e., high, intermediate, and inactive) of sites exist in all materials, and the difference in catalytic activity can be attributed to the difference in the fraction of each type of sites with limited to no micropore materials having the greatest fraction of active sites. MD simulations and NMR experiments provide evidence to support the hypothesis that the inactive sites are located in the micropores. Reducing the micropore volume increases the catalytic activity for additional reactions promoted by amine-silanol interactions (i.e., Knoevenagel condensation) and hindered by amine-silanol interactions (i.e., glucose isomerization). Overall, the results demonstrate the benefit of reducing the micropore volume to achieve highly active aminosilica materials.

#### **Declaration of Competing Interest**

The authors declare that they have no known competing financial interests or personal relationships that could have appeared to influence the work reported in this paper.

#### Acknowledgements

N.D. and N.A.B. gratefully acknowledge the American Chemical Society Petroleum Research Fund (ACS-PRF 55946-DNI5), the National Science Foundation (NSF 1653587 and 2015669), and the Ohio State University Institute for Materials Research (OSU IMR FG0211 and EMR-G00018) for their financial support. The authors also thank the computational resources provided by the Ohio Supercomputer Center (OSC). Solid-state NMR experiments (Backspace(TK) were supported by the U.S. Department of Energy (DOE), Office of Basic Energy Sciences, Chemical Sciences, Geo-

sciences, and Biosciences Division. The research was performed at the Ames Laboratory, which is operated for the U.S. DOE by Iowa State University under contract # DE-AC02-07CH11358.

#### Appendix A. Supplementary material

Supplementary data to this article can be found online at https://doi.org/10.1016/j.jcat.2022.09.016.

#### References

- [1] V.-S.-Y. Lin, C.Y. Lai, J. Huang, S.A. Song, S. Xu, Molecular recognition inside of multifunctionalized mesoporous silicas: toward selective fluorescence detection of dopamine and glucosamine, J. Am. Chem. Soc. 123 (2001) 11510–11511, https://doi.org/10.1021/ja016223m.
- [2] S. Yuan, M. Wang, J. Liu, B. Guo, Recent advances of SBA-15-based composites as the heterogeneous catalysts in water decontamination: a mini-review, J. Environ. Manage. 254 (2020) 109787, https://doi.org/10.1016/ j.jenvman.2019.109787.
- [3] J.C. Hicks, J.H. Drese, D.J. Fauth, M.L. Gray, G. Qi, C.W. Jones, Designing Adsorbents for CO2 capture from flue gas-hyperbranched aminosilicas capable of capturing CO2 reversibly, J. Am. Chem. Soc. 130 (2008) 2902, https://doi.org/ 10.1021/ja077795v.
- [4] Y. Kuwahara, D.-Y. Kang, J.R. Copeland, N.A. Brunelli, S.A. Didas, P. Bollini, C. Sievers, T. Kamegawa, H. Yamashita, C.W. Jones, Dramatic enhancement of CO2 uptake by poly(ethyleneimine) using zirconosilicate supports, J. Am. Chem. Soc. 134 (2012), https://doi.org/10.1021/ja303136e.
- [5] M. Vallet-Regí, F. Balas, D. Arcos, Mesoporous materials for drug delivery, Angew. Chem. - Int. Ed. 46 (2007) 7548–7558, https://doi.org/10.1002/ anie 200604488
- [6] M. Vallet-Regi, A. Rámila, R.P. Del Real, J. Pérez-Pariente, A new property of MCM-41: drug delivery system, Chem. Mater. 13 (2001) 308–311, https://doi. org/10.1021/cm0011559.
- [7] V. Fathi Vavsari, G. Mohammadi Ziarani, A. Badiei, The role of SBA-15 in drug delivery, RSC Adv. 5 (2015) 91686–91707, https://doi.org/10.1039/ c5ra17780d.
- [8] R. Métivier, I. Leray, B. Lebeau, B. Valeur, A mesoporous silica functionalized by a covalently bound calixarene-based fluoroionophore for selective optical sensing of mercury(II) in water, J. Mater. Chem. 15 (2005) 2965–2973, https:// doi.org/10.1039/b501897b.
- [9] J. He, X. Li, D.G. Evans, X. Duan, C. Li, A new support for the immobilization of penicillin acylase, J. Mol. Catal. - B Enzym. 11 (2000) 45–53, https://doi.org/ 10.1016/S1381-1177(00)00218-6.
- [10] P. Verma, Y. Kuwahara, K. Mori, R. Raja, H. Yamashita, Functionalized mesoporous SBA-15 silica: recent trends and catalytic applications, Roy. Soc. Chem. (2020), https://doi.org/10.1039/d0nr00732c.
- [11] A. Cauvel, G. Renard, D. Brunel, Monoglyceride synthesis by heterogeneous catalysis using MCM-41 type silicas functionalized with amino groups, J. Org. Chem. 62 (1997) 749–751, https://doi.org/10.1021/jo9614001.
- [12] D. Brunel, Functionalized micelle-templated silicas (MTS) and their use as catalysts for fine chemicals, Micropor. Mesopor. Mater. 27 (1999) 329–344, https://doi.org/10.1016/S1387-1811(98)00266-2.
- [13] N.A. Brunelli, C.W. Jones, Tuning acid-base cooperativity to create next generation silica-supported organocatalysts, J. Catal. 308 (2013) 60–72, https://doi.org/10.1016/j.jcat.2013.05.022.
- [14] N.A. Brunelli, S.A. Didas, K. Venkatasubbaiah, C.W. Jones, Tuning cooperativity by controlling the linker length of silica-supported amines in catalysis and CO2 capture, J. Am. Chem. Soc. 134 (2012) 13950–13953, https://doi.org/ 10.1021/ja305601g.
- [15] N.A. Brunelli, K. Venkatasubbaiah, C.W. Jones, Cooperative catalysis with acid-base bifunctional mesoporous silica: impact of grafting and co-condensation synthesis methods on material structure and catalytic properties, Chem. Mater. 24 (2012) 2433–2442, https://doi.org/10.1021/cm300753z.
- [16] K. Ponnuru, J.C. Manayil, H.J. Cho, W. Fan, K. Wilson, F.C. Jentoft, Intraparticle diffusional versus site effects on reaction pathways in liquid-phase cross aldol reactions, ChemPhysChem 19 (2018) 386–401, https://doi.org/10.1002/ cphc.201701219.
- [17] M. Ide, M. El-Roz, E. De Canck, A. Vicente, T. Planckaert, T. Bogaerts, I. Van Driessche, F. Lynen, V. Van Speybroeck, F. Thybault-Starzyk, P. Van Der Voort, Quantification of silanol sites for the most common mesoporous ordered silicas and organosilicas: total versus accessible silanols, Phys. Chem. Chem. Phys. 15 (2013) 642–650, https://doi.org/10.1039/c2cp42811c.
- [18] E.G. Moschetta, N.A. Brunelli, C.W. Jones, Reaction-dependent heteroatom modification of acid-base catalytic cooperativity in aminosilica materials, Appl. Catal. A, Gen. 504 (2015) 429–439, https://doi.org/10.1016/j. apcata.2014.10.061.
- [19] R.K. Zeidan, S.-J. Hwang, M.E. Davis, Multifunctional heterogeneous catalysts: SBA-15-containing primary amines and sulfonic acids, Angew. Chem. Int. Ed. 45 (2006) 6332–6335, https://doi.org/10.1002/anie.200602243.
- [20] R.K. Zeidan, M.E. Davis, The effect of acid-base pairing on catalysis: an efficient acid-base functionalized catalyst for aldol condensation, J. Catal. 247 (2007) 379–382, https://doi.org/10.1016/j.jcat.2007.02.005.

- [21] J.D. Bass, A. Solovyov, A.J. Pascall, A. Katz, Acid-base bifunctional and dielectric outer-sphere effects in heterogeneous catalysis: a comparative investigation of model primary amine catalysts, J. Am. Chem. Soc. 128 (2006) 3737–3747, https://doi.org/10.1021/ja057395c.
- [22] J.D. Bass, S.L. Anderson, A. Katz, The effect of outer-sphere acidity on chemical reactivity in a synthetic heterogeneous base catalyst, Angew. Chem. Int. Ed. 115 (2003) 5377–5380, https://doi.org/10.1002/ange.200352181.
- [23] K.M. Chepiga, Y. Feng, N.A. Brunelli, C.W. Jones, H.M.L. Davies, Silicaimmobilized chiral dirhodium(II) catalyst for enantioselective carbenoid reactions, Org. Lett. 15 (2013) 6136–6139, https://doi.org/10.1021/ pl403006r
- [24] E.G. Moschetta, S. Negretti, K.M. Chepiga, N.A. Brunelli, Y. Labreche, Y. Feng, F. Rezaei, R.P. Lively, W.J. Koros, H.M.L. Davies, C.W. Jones, Composite polymer/oxide hollow fiber contactors: versatile and scalable flow reactors for heterogeneous catalytic reactions in organic synthesis, Angew. Chem. Int. Ed. 54 (2015) 6470–6474, https://doi.org/10.1002/anie.201500841.
- [25] A.J. Crisci, M.H. Tucker, M.Y. Lee, S.G. Jang, J.A. Dumesic, S.L. Scott, Acid-functionalized SBA-15-type silica catalysts for carbohydrate dehydration, ACS Catal. 1 (2011) 719–728, https://doi.org/10.1021/cs2001237.
- [26] J. Huo, R.L. Johnson, P. Duan, H.N. Pham, D. Mendivelso-Perez, E.A. Smith, A.K. Datye, K. Schmidt-Rohr, B.H. Shanks, Stability of Pd nanoparticles on carbon-coated supports under hydrothermal conditions, Catal. Sci. Technol. 8 (2018) 1151–1160, https://doi.org/10.1039/c7cy02098h.
- [27] F. Shang, S. Wu, J. Guan, J. Sun, H. Liu, C. Wang, Q. Kan, A comparative study of aminopropyl-functionalized SBA-15 prepared by grafting in different solvents, Reac. Kinet. Mech. Cat. 103 (2011) 181–190, https://doi.org/10.1007/s11144-011-0290-7.
- [28] W. Xu, S. Ji, W. Quan, J. Yu, One-Pot Synthesis of Dimethyl Carbonate over Basic Zeolite Catalysts 2013 (2013) 22–27.
- [29] B. List, R.A. Lerner, C.F. Barbas III, Proline-catalyzed direct asymmetric aldol reactions, J. Am. Chem. Soc. 122 (2000) 2395–2396, https://doi.org/ 10.1021/ja994280v.
- [30] A.B. Northrup, D.W.C. MacMillan, The first direct and enantioselective crossaldol reaction of aldehydes, J. Am. Chem. Soc. 124 (2002) 6798–6799, https:// doi.org/10.1021/ja0262378.
- [31] N. Deshpande, L. Pattanaik, M.R. Whitaker, C.-T. Yang, L.-C. Lin, N.A. Brunelli, Selectively converting glucose to fructose using immobilized tertiary amines, J. Catal. 353 (2017) 205–210, https://doi.org/10.1016/j.jcat.2017.07.021.
- [32] N. Deshpande, E.H. Cho, A.P. Spanos, L.-C. Lin, N.A. Brunelli, Tuning molecular structure of tertiary amine catalysts for glucose isomerization, J. Catal. 372 (2019) 119–127, https://doi.org/10.1016/j.jcat.2019.02.025.
- [33] Y. Kubota, K. Goto, S. Miyata, Y. Goto, Y. Fukushima, Y. Sugi, Enhanced effect of mesoporous silica on base-catalyzed aldol reaction, Chem. Lett. 32 (2003) 234-235, https://doi.org/10.1246/cl.2003.234.
- [34] Q. Wang, V.V. Guerrero, A. Ghosh, S. Yeu, J.D. Lunn, D.F. Shantz, Catalytic properties of dendron-OMS hybrids, J. Catal. 269 (2010) 15–25, https://doi.org/ 10.1016/j.jcat.2009.10.009.
- [35] S.L. Hruby, B.H. Shanks, Acid-base cooperativity in condensation reactions with functionalized mesoporous silica catalysts, J. Catal. 263 (2009) 181–188, https://doi.org/10.1016/j.jcat.2009.02.011.
- [36] J. Lauwaert, E. De Canck, D. Esquivel, J.W. Thybaut, P. Van Der Voort, G.B. Marin, Silanol-assisted aldol condensation on aminated silica: Understanding the arrangement of functional groups, ChemCatChem 6 (2014) 255–264, https://doi.org/10.1002/cctc.201300742.
- [37] N.A. Brunelli, C.W. Jones, Tuning acid-base cooperativity to create next generation silica-supported organocatalysts, J. Catal. 308 (2013) 60-72, https://doi.org/10.1016/j.jcat.2013.05.022.
- [38] F.R. Clemente, K.N. Houk, Computational evidence for the enamine mechanism of intramolecular aldol reactions catalyzed by proline, Angew. Chemie. 116 (2004) 5890–5892, https://doi.org/10.1002/ange.200460916.
- [39] K. Kandel, S.M. Althaus, C. Peeraphatdit, T. Kobayashi, B.G. Trewyn, M. Pruski, I. I. Slowing, Solvent-induced reversal of activities between two closely related heterogeneous catalysts in the aldol reaction, ACS Catal. 3 (2013) 265–271, https://doi.org/10.1021/cs300748g.
- [40] B. List, L. Hoang, H.J. Martin, New mechanistic studies on the proline-catalyzed aldol reaction, Proc. Nat. Acad. Sci. 101 (2004) 5839–5842, https://doi.org/ 10.1073/pnas.0307979101.
- [41] J. Lauwaert, E.G. Moschetta, P. Van Der Voort, J.W. Thybaut, C.W. Jones, G.B. Marin, Spatial arrangement and acid strength effects on acid-base cooperatively catalyzed aldol condensation on aminosilica materials, J. Catal. 325 (2015) 19–25, https://doi.org/10.1016/j.jcat.2015.02.011.
- [42] S. Shylesh, D. Hanna, J. Gomes, C.G. Canlas, M. Head-Gordon, A.T. Bell, The role of hydroxyl group acidity on the activity of silica-supported secondary amines for the self-condensation of n-butanal, ChemSusChem 8 (2015) 466–472, https://doi.org/10.1002/cssc.201402443.
- [43] S. Nedd, T. Kobayashi, C.H. Tsai, I.I. Slowing, M. Pruski, M.S. Gordon, Using a reactive force field to correlate mobilities obtained from solid-state 13C NMR on mesoporous silica nanoparticle systems, J. Phys. Chem. C. 115 (2011) 16333–16339, https://doi.org/10.1021/jp204510m.

- [44] M. Kruk, M. Jaroniec, C.H. Ko, R. Ryoo, Characterization of the porous structure of SBA-15, Chem. Mater. 12 (2000) 1961–1968, https://doi.org/10.1021/ cm000164e.
- [45] A. Galarneau, H. Cambon, F. Renzo, R. Ryoo, M. Choi, F. Fajula, Microporosity and connections between pores in SBA-15 mesostructured silicas as a function of the temperature of synthesis, New J. Chem. 27 (2003) 73–79, https://doi. org/10.1039/B207378C.
- [46] K. Flodström, V. Alfredsson, Influence of the block length of triblock copolymers on the formation of mesoporous silica, Micropor. Mesopor. Mater. 59 (2003) 167–176, https://doi.org/10.1016/S1387-1811(03)00308-1.
- [47] S. Wu, Y. Han, Y.C. Zou, J.W. Song, L. Zhao, Y. Di, S.Z. Liu, F.S. Xiao, Synthesis of heteroatom substituted SBA-15 by the "pH-Adjusting" method, Chem. Mater. 16 (2004) 486-492, https://doi.org/10.1021/cm0343857.
- [48] S. Singh, R. Kumar, H.D. Setiabudi, S. Nanda, D.V.N. Vo, Advanced synthesis strategies of mesoporous SBA-15 supported catalysts for catalytic reforming applications: a state-of-the-art review, Appl. Catal. A, Gen. 559 (2018) 57–74, https://doi.org/10.1016/j.apcata.2018.04.015.
- [49] R. Lin, G. Carlström, Q. Dat Pham, M.W. Anderson, D. Topgaard, K.J. Edler, V. Alfredsson, Kinetic influence of siliceous reactions on structure formation of mesoporous silica formed via the co-structure directing agent route, J. Phys. Chem. C. 120 (2016) 3814–3821, https://doi.org/10.1021/acs.jpcc.5b11348.
- [50] T. Kjellman, V. Alfredsson, The use of in situ and ex situ techniques for the study of the formation mechanism of mesoporous silica formed with non-ionic triblock copolymers, Chem. Soc. Rev. 42 (2013) 3777–3791, https://doi.org/ 10.1039/c2cs35298b.
- [51] T. Kjellman, N. Reichhardt, M. Sakeye, J.H. Smaištt, M. Lindén, V. Alfredsson, Independent fine-tuning of the intrawall porosity and primary mesoporosity of SBA-15, Chem. Mater. 25 (2013) 1989–1997, https://doi.org/10.1021/ cm4009442
- [52] R.A. Pollock, B.R. Walsh, J. Fry, I.T. Ghampson, Y.B. Melnichenko, H. Kaiser, R. Pynn, W.J. Desisto, M.C. Wheeler, B.G. Frederick, Size and spatial distribution of micropores in SBA-15 using CM-SANS, Chem. Mater. 23 (2011) 3828–3840, https://doi.org/10.1021/cm200707y.
- [53] R.A. Pollock, G.Y. Gor, B.R. Walsh, J. Fry, I.T. Ghampson, Y.B. Melnichenko, H. Kaiser, W.J. Desisto, M.C. Wheeler, B.G. Frederick, Role of liquid vs vapor water in the hydrothermal degradation of SBA-15, J. Phys. Chem. C. 116 (2012) 22802–22814, https://doi.org/10.1021/jp303150e.
- [54] A. Kane, N. Deshpande, N.A. Brunelli, Impact of surface loading on catalytic activity of regular and low micropore SBA-15 in the Knoevenagel condensation, AIChE J. 65 (2019) e16791, https://doi.org/10.1002/aic.16791.
- [55] J.-Y. Chen, N.A. Brunelli, Investigating the impact of microporosity of aminosilica catalysts in aldol condensation reactions for biomass upgrading of 5-hydroxymethylfurfural and furfuraldehyde to fuels, Energy Fuels 35 (2021) 14885–14893, https://doi.org/10.1021/acs.energyfuels.1c01934.
- [56] D. Zhao, J. Feng, Q. Huo, N. Melosh, G.H. Fredrickson, B.F. Chmelka, G.D. Stucky, Triblock copolymer syntheses of mesoporous silica with periodic 50 to 300 angstrom pores, Science (80-.). 279 (1998) 548–552. doi:10.1126/science.279.5350.548.
- [57] H.-T. Chen, S. Huh, J.W. Wiench, M. Pruski, V.-S.-Y. Lin, Dialkylaminopyridinefunctionalized mesoporous silica nanosphere as an efficient and highly stable heterogeneous nucleophilic catalyst, J. Am. Chem. Soc. 127 (2005) 13305– 13311. http://www.ncbi.nlm.nih.gov/pubmed/16173762.
- [58] J.M. Kim, J.H. Kwak, S. Jun, R. Ryoo, Ion exchange and thermal stability of MCM-41, J. Phys. Chem. 99 (1995) 16742–16747, https://doi.org/10.1021/ i100045a039.
- [59] J.M. Kim, R. Ryoo, Disintegration of mesoporous structures of MCM-41 and MCM-48 in water, Bull. Korean Chem. Soc. 17 (1996) 66–68.
- [60] C. Chen, H. Li, M.E. Davis, Studies on mesoporous materials I. Synthesis and characterization of MCM-41, Micropor. Mater. 2 (1993) 17–26, https://doi.org/ 10.1016/0927-6513(93)80058-3.
- [61] B.R. Goldsmith, B. Peters, J.K. Johnson, B.C. Gates, S.L. Scott, Beyond ordered materials: understanding catalytic sites on amorphous solids, ACS Catal. 7 (2017) 7543–7557, https://doi.org/10.1021/acscatal.7b01767.
- [62] N.A. Brunelli, W. Long, K. Venkatasubbaiah, C.W. Jones, Catalytic regioselective epoxide ring opening with phenol using homogeneous and supported analogues of dimethylaminopyridine, Top. Catal. 55 (2012) 432–438, https:// doi.org/10.1007/s11244-012-9822-2
- [63] J.-Y. Chen, H. Pineault, N.A. Brunelli, Quantifying the impact of surface density of aminosilanes on the fraction of active sites in SBA-15 for the Aldol reaction and condensation, J. Catal. (2022).
- [64] G. Li, B. Wang, T. Kobayashi, M. Pruski, D.E. Resasco, Optimizing the surface distribution of acid sites for cooperative catalysis in condensation reactions promoted by water, Chem Catal. 1 (2021) 1065–1087, https://doi.org/10.1016/ j.checat.2021.08.005.
- [65] C. Pirez, J.C. Morin, J.C. Manayil, A.F. Lee, K. Wilson, Sol-gel synthesis of SBA-15: Impact of HCl on surface chemistry, Micropor. Mesopor. Mater. 271 (2018) 196–202, https://doi.org/10.1016/j.micromeso.2018.05.043.